Electric field gradient and its temperature variation at ^{111}Cd in ruthenium and osmium

L. Hermans, M. Rots, and J. Vancauteren
Instituut voor Kern- en Stralingsfysika, B-3030 Leuven, Belgium
(Received 20 December 1982)

The nuclear quadrupole interaction at ^{111}Cd in Ru and Os was measured as a function of temperature with the use of the γ-γ perturbed angular correlation technique. The temperature variation of the electric field gradient is very small for each of the host materials but follows the $T^{3/2}$ law. The present results are discussed in comparison with our earlier measurements of the electric field gradient at ^{111}Cd in the other transition metals Ti, Zr, Hf, and Re.

I. INTRODUCTION

Nowadays the temperature variation of the electric field gradient (EFG) in nontransition metals is well documented and the data can be represented by the empirical relation

$$eq(T)=eq(0)(1-BT^{3/2}) \tag{1}$$

with B the so-called slope parameter.[1] Recent experiments show that B is roughly proportional to $(M\Theta_D^2)^{-1}$ (Θ_D is the Debye temperature of the host lattice, M is the mass of a host atom) not only for pure systems but also for impurity systems.[2,3] Nishiyama and Riegel[4] found that the combination of the lattice expansion and the $T^{3/2}$ dependence of the mean-square displacement $\langle x^2\rangle$ results in a $T^{3/2}$ law for the EFG. It is important to note here that a $T^{3/2}$ dependence of $\langle x^2\rangle$ is empirical and, although not reproducible analytically, it is very well approximated in the framework of a quasiharmonic theory.[5] The repopulation of the electronic states at the Fermi level has little influence on the EFG for normal metals. For some transition metals, however, electronic effects may be strong, resulting in a deviation from the $T^{3/2}$ law.

Unfortunately, the variation of the EFG as a function of temperature in a pure transition metal has not been measured until now, but there exist experimental data on what we will call almost pure systems, e.g., ^{44}Sc*Ti* (Ref. 6) and ^{181}Ta*Hf* (Ref. 7). The electronic structure of the impurity core is very similar to the structure of the host atom core; therefore, we may consider the temperature dependence of the EFG for ^{44}Sc*Ti* and ^{181}Ta*Hf* as representative of the pure systems. The experimental results indicate that these almost pure systems do follow the $T^{3/2}$ law, with a slope parameter B proportional to $(M\Theta_D^2)^{-1}$, in line with nontransition metals.

This observation is opposite to what was found in a limited number of impurity-transition-metal systems. There, in most cases, a strongly probe-dependent temperature variation of the EFG was found not following the $T^{3/2}$ law. The present results on the temperature dependence of the EFG at ^{111}Cd in Ru and Os complete a series of experiments[8,9] performed on the same impurity in different hexagonal transition-metal hosts. With the use of the data presently available we will look for systematic trends.

II. EXPERIMENTAL

The applied experimental technique is time-differential perturbed angular correlations (TDPAC) on the familiar ^{111}Cd cascade and we refer to previous work for details.[8,9] Both the sources were prepared by room-temperature implantation of the ^{111}In parent activity, at an energy of 85 keV, into Ru and Os single crystals. The Ru and Os crystals were implanted to a dose of 2×10^{13} and 1×10^{13} atoms/cm^2, respectively. After implantation the Ru and Os crystals were annealed at 800°C for 22 and 10 h, respectively, under a high-purity (99.9999%) dried argon atomsphere. During annealing a considerable part of the activity was evaporated from both the samples.

The samples had to be annealed because the TDPAC spectra of the as-implanted samples did not show up the pattern expected for a well-defined nuclear quadrupole interaction. After the heat treatment a pattern corresponding to an almost undamped unique nuclear quadrupole interaction appears, showing that almost all nuclei are sensing the same electric field gradient. The ^{111}In impurity concentration was estimated to be 100 ppm for Os and 200 ppm for the Ru sample. A conventional four-detector setup with four 1.5 in.$\times$1.5 in. NaI(Tl) scintillation crystals mounted on RCA 8575 photomultipliers coupled to a fast-slow coincidence counting system was used for data collection. With the single-channel analyzers gated on the appropriate γ rays a time resolution of typical 2.5 nsec was obtained. Data collection and reduction are extensively discussed in previous reports.[8,9] For the intermediate 247-keV level with spin $I=\frac{5}{2}$ in ^{111}Cd the time evolution of the correlation anisotropy under the influence of a static and axially symmetric quadrupole interaction ($\eta=0$) is given by

$$R(t)=\sum_{n=0}^{3} S_n \exp[-\tfrac{1}{2}(n\omega_0\sigma t)^2]\cos(n\omega_0 t)\ .$$

The frequency ω_0 is related to the nuclear quadrupole coupling constant ν_q through

$$\omega_0=\frac{3\Pi}{I(2I-1)}\nu_q,\quad \nu_q=\frac{e^2qQ}{h}$$

where Q is the nuclear quadrupole moment and eq the largest component of the EFG tensor in the principal-axis system.

The exponential factors allow for a possible Gaussian distribution of the EFG's around the value ω_0 with a width σ. The orientation of the Os single crystal was known to be perpendicular to the surface of the single-crystal disk. The Ru single crystal was cut from a single-crystal bar perpendicular to the cylinder axis. Usually the

c axis is parallel to that axis. We oriented the crystals so that the c axis was in the plane of the detectors at a 45° angle to either of them. In all the fitting procedures the coefficients S_n were free, allowing for possible texture in the single crystal. The time resolution is small compared to the time period of the quadrupole interaction frequency and is therefore disregarded in the data analysis with S_n, ω_0, and σ as the only free parameters.

III. RESULTS

A. ^{111}Cd*Ru*

The spin precession spectra observed are shown in Fig. 1. The nuclear quadrupole interaction frequency $\nu_q = 22.6(3)$ MHz at 293 K. All the spectra could be fitted with $\eta = 0$. The amplitudes are slightly attenuated. The spread in EFG's i.e., σ has a maximum value of 0.07(1) for the measurement at 4.2 K and reduces to a minimum value 0.03(1) at the highest measuring temperature $T = 1080$ K. Radiation damage still present after the given heat treatment seems to anneal out further during data collection at high temperatures. The spectra show neither the pattern expected for a single crystal in the present geometry nor the pattern expected for a polycrystalline sample. We checked the crystal structure by the Laue back-reflection technique and observed rings and well-defined points of increased intensity, showing that there are polycrystalline parts in our crystal. We believe that these parts are situated on the surface and are produced during mechanical polishing after cutting. We also found that the c axis of the single crystal part is not perpendicular to the cutting plane.

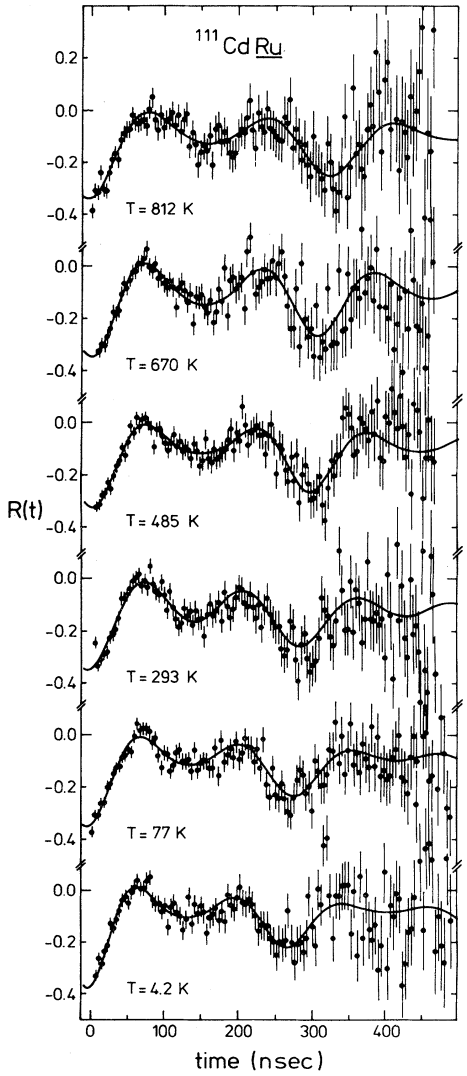

FIG. 1. Spin precession spectra for the nuclear quadrupole interaction at ^{111}Cd in Ru for different temperatures.

TABLE I. The observed quadrupole interaction frequency ν_q at ^{111}Cd in Ru at different temperatures. eq_{expt} is the electric field gradient. eq_{ion} and eq_{el} are the ionic and electronic contributions as detailed in the text.

T (K)	ν_q (MHz)	eq_{expt} (10^{17} V/cm^2)	eq_{ion} (10^{17} V/cm^2)	eq_{el} ($eq_{\text{expt}} < 0$) (10^{17} V/cm^2)
4.2	24.6(3)	1.27(11)	+2.05	−3.32
77	23.7(3)	1.23(11)	+2.04	−3.27
293	22.6(3)	1.17(10)	+2.00	−3.17
485	22.4(3)	1.16(10)	+1.97	−3.13
670	21.5(2)	1.11(10)	+1.92	−3.03
812	20.5(2)	1.06(9)	+1.89	−2.95
1080	19.6(2)	1.01(9)	+1.81	−2.82

Using the nuclear quadrupole moment [$Q = 0.80(7)b$] (Ref. 10) we calculated eq_{expt} as listed in Table I. The large error on eq_{expt} is almost entirely due to the uncertainty of the value of Q.

Usually one separates the EFG contributions in eq_{el} due to the conduction electrons and eq_{ion} due to the lattice ions. The lattice contribution at the bare nucleus obtained from the formula of Das and Pomerantz[11] is multiplied by the Sternheimer antishielding factor $(1-\gamma_\infty)$ to account for the deformation of the core electron cloud by the external charges. Feiock and Johnson[12] calculated $\gamma_\infty = 29.3$ for the Cd^{2+} charge state.

Using the measured lattice constants of Ru (Refs. 13 and 14) and assuming a +4 charge state of the Ru lattice ions we obtain the eq_{ion} values listed in Table I. Accord-

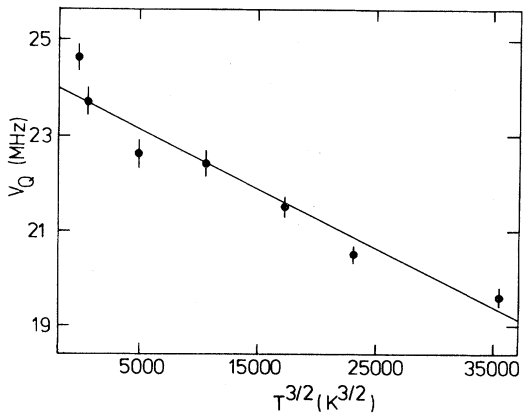

FIG. 2. Quadrupole interaction frequency ν_q vs $T^{3/2}$ for ^{111}Cd*Ru*.

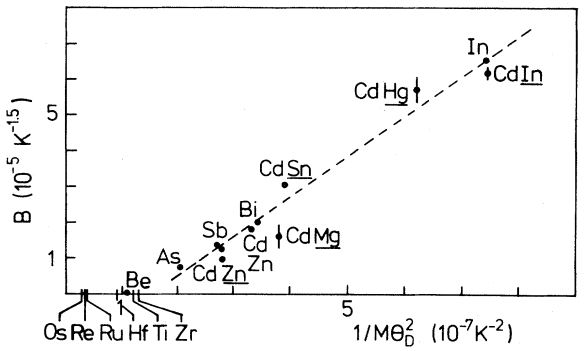

FIG. 3. Slope parameter B vs $(M\Theta_D^2)^{-1}$ for different systems.

ing to the universal correlation[15] we take eq_{expt} negative and calculate the enhancement factor $K=eq_{\text{el}}/eq_{\text{ion}}=-1.5$. The quadrupole interaction strength ν_q vs $T^{3/2}$ is displayed in Fig. 2.

The solid curve represents a $T^{3/2}$ dependence as

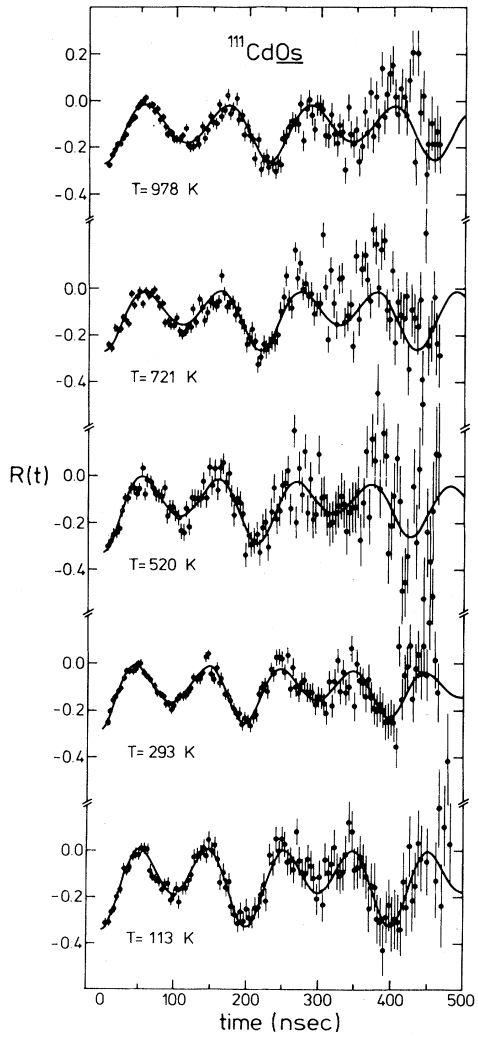

FIG. 4. Spin precession spectra for the nuclear quadrupole interaction at ^{111}Cd in Os at different temperatures.

TABLE II. The observed quadrupole interaction frequency ν_q at ^{111}Cd in Os at different temperatures. eq_{expt} is the electric field gradient. eq_{ion} and eq_{el} are the ionic and electronic contributions as detailed in the text.

T (K)	ν_q (MHz)	eq_{expt} (10^{17} V/cm^2)	eq_{ion} (10^{17} V/cm^2)	eq_{el} ($eq_{\text{expt}}<0$) (10^{17} V/cm^2)
113	33.5(3)	1.73(15)	+2.10	−3.83
293	33.4(3)	1.72(15)	+2.06	−3.78
520	31.4(3)	1.62(14)	+2.03	−3.65
721	30.7(3)	1.58(14)	+2.00	−3.58
978	29.2(3)	1.51(13)	+1.95	−3.46

$$\nu_q(T)=\nu_q(0)(1-BT^{3/2})$$

with $\nu_q(0)=23.7(3)$ MHz and $B=0.53(4)\times10^{-5}$ K$^{-3/2}$. If the temperature dependence of the EFG is entirely due to lattice effects, as suggested by the $T^{3/2}$ law, B should be proportional to $(M\Theta_D^2)^{-1}$ with the same proportionality constant as found for nontransition metals (Fig. 3). With the Debye temperature of Ru, $\Theta_D=554$ K, we find $(M\Theta_D^2)^{-1}=0.3\times10^{-7}$ K^{-2} and we infer from Fig. 3 that indeed B must be smaller than 10^{-5} K$^{-3/2}$.

B. ^{111}Cd*Os*

The nuclear quadrupole interaction frequency $\nu_q=31.5(2)$ MHz at 293 K. This value is half the value reported by Recknagel *et al.*[16] ($\nu_q=65$ MHz). Their value represents $2\nu_q$ (Ref. 17) instead of ν_q so that the two experiments are in good agreement.

The spectra observed are shown in Fig. 4. Here also the pattern does not correspond to the one expected for a single crystal in our detection geometry. Probably the surface structure of the Os single crystal was partially destroyed during mechanical polishing to remove previously implanted impurities. The amplitudes of the spin precession spectra are undamped and all spectra could be fitted with $\eta=0$. We calculated eq_{expt}, eq_{ion}, and eq_{el} as tabulated in Table II.

We used for the lattice constants interpolated and extrapolated values from measurements of Finkel *et al.*[14] between 77 and 300 K and of Owen and Roberts[18] between 293 and 973 K. We assumed that Os lattice ions to be in a +4 charge state. If we take a negative sign for eq_{expt}, as

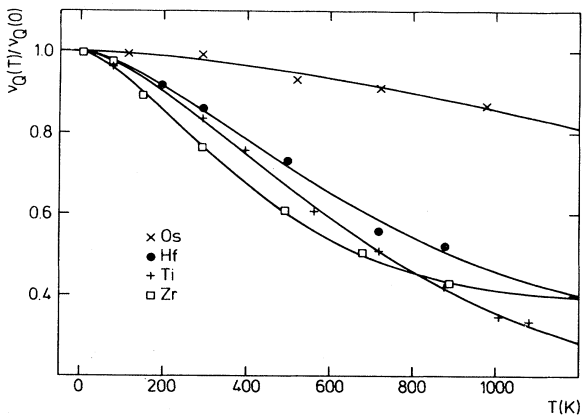

FIG. 5. Quadrupole interaction frequency ν_q vs T for ^{111}Cd in Os, Ti, Zr, and Hf.

TABLE III. Results from the fit of the experimental EFG data at ^{111}Cd in Ti, Zr, and Hf to a function $c+a\exp(-B'T^{3/2})$.

Host	a (MHz)	c (MHz)	B' (10^{-5} K$^{-3/2}$)	$B''=\left[\frac{a}{a+c}\right]B'$ (10^{-5} K$^{-3/2}$)
Ti	28.6(4)	4.8(4)	4.4(1)	3.8(1)
Zr	12.0(3)	7.4(3)	9.2(5)	5.6(4)
Hf	23.7(5)	9.9(5)	4.5(5)	3.2(4)

suggested by the universal correlation, we find $K=-1.8$.

The values of ν_q at different temperatures plotted against T (Fig. 5) follow a $T^{3/2}$ dependence with $\nu_q(0)=33.7$ MHz and $B=0.45\times10^{-5}$ K$^{-3/2}$. The value $(M\Theta_D^2)^{-1}=0.28\ 10^{-7}$ K^{-2} calculated with $\Theta_D=431$ K is located in Fig. 3 showing that B should be smaller than 10^{-5} K$^{-3/2}$ if the temperature dependence is entirely due to lattice effects. Our result confirms that for the case ^{111}Cd*Os* the linear relation between B and $(M\Theta_D^2)^{-1}$ holds.

IV. DISCUSSION

The theory of Nishiyama and Riegel shows that there must exist a correlation between lattice expansion and lattice vibration in order to explain the $T^{3/2}$ law of the EFG in pure materials. The existence of this correlation can be understood from the fact that both lattice expansion and vibration of a lattice atom are a function of the same interatomic potential. For pure systems deviations from the $T^{3/2}$ law may be expected in those cases where electronic effects contribute significantly to the temperature dependence of the EFG.

The temperature dependence at an impurity, however, should be influenced considerably by the change in interatomic force constants.[19] If the force constants are not much affected and electronic effects are small the slope parameter B should be proportional to $(M\Theta_D^2)^{-1}$ even for transition-metal hosts. The experimental data on ^{44}Sc*Ti* and ^{181}Ta*Hf* can be fitted to a $T^{3/2}$ dependence with B values proportional to the appropriate $(M\Theta_D^2)^{-1}$ values. This shows us that for the almost pure, and very likely also for the pure systems, the electronic contribution to the temperature variation of the EFG is small. The present results on ^{111}Cd in Ru and Os also show a $T^{3/2}$ dependence of the EFG with B proportional to $(M\Theta_D^2)^{-1}$. The EFG at ^{111}Cd in Re did not follow the $T^{3/2}$ law although the changes with temperature were of the expected order of magnitude. Moreover, the EFG at ^{181}Ta in Re (Ref. 20) also showed little temperature variation.

All these results suggest that electronic effects are not very important in comparison to lattice-dynamical effects in Re, Os, and Ru. In addition, the vibrational properties of the Cd impurity are closely related to those of the pure material, which means that the Cd atom is strongly bound to the host lattice.

These observations are in strong contrast to what we measured for the group-IV*A* group metals Ti, Zr, and Hf.[8,9] The temperature dependence of the EFG at ^{111}Cd is much stronger than expected from the correlation with $(M\Theta_D^2)^{-1}$ for the pure systems. The data on ^{111}Cd in Ti, Zr, and Hf suggest that the Cd atoms are weakly bound to the host lattice, implying that the correlation between lattice expansion (bulk property) and impurity vibration ($\langle x^2\rangle$) is lost.

For the special case in which the contributions of lattice expansion are relatively small compared to vibrational effects, the theory of Nishiyama and Riegel implies that the temperature variation should follow a $\exp(-T^{3/2})$ dependence. To test this we fitted our data on ^{111}Cd in Ti, Zr, and Hf to a $c+a\exp(-B'T^{3/2})$ function. The results are listed in Table III and Fig. 5. The fits are surprisingly good considering the fact that we ignored the influence from lattice expansion completely. The B' values are not directly comparable to the B values of the $T^{3/2}$ law. For small T values one can expand $\exp(-B'T^{3/2})$ in a Taylor series and our fit function can then be written as $(c+a)(1-B''T^{3/2})$ with $B''=[a/(c+a)]B'$. The B'', comparable with B values, are listed in Table III. We see that the B'' values are among the largest ever measured.

The question arises how to explain the large difference in force constants between the Cd impurity and the surrounding lattice comparing the group-IV*A* metals Ti, Zr, and Hf with Ru, Os, and Re. Rafailovich and Schatz[21] showed that there exists a proportionality between the host-to-impurity force-constant ratio and the host-to-impurity volume ratio. Therefore, we have listed in Table IV the atomic radii and compressibilities of the metals of interest. And indeed the Cd atom has to be compressed considerably to fit in a Ru, Os, or Re lattice, whereas only little compression is necessary for Ti and no compression for Zr and Hf. But as can be seen in Table IV there is also

TABLE IV. Atomic diameter (D), compressibility (β_V) at 300 K, and electron density at the boundary of the Wigner-Seitz cell (n_{WS}) of the hexagonal transition metals and Cd.

	Ti	Zr	Hf	Ru	Re	Os	Cd
D (Å)[a]	2.894	3.179	3.127	2.650	2.740	2.675	2.979
β_V (10^{-12} cm^2/dyn)	0.931[b]	1.050[b]	0.918[b]	0.318[c]	0.272[c]	0.27[d]	2.17[e]
n_{WS} (10^{-2} electrons/a.u.^{3})	3.2[f]	2.5[f]	2.9[f]	6.5[f]	6.5[f]	6.7[f]	2.00[g]

[a]All data from W. Hume-Rothery, R. E. Smallman, and C. W. Haworth, *The Structure of Metals and Alloys* (Institute of Metals, London, 1969).
[b]E. S. Fisher and C. J. Renken, Phys. Rev. 135, A482 (1964).
[c]E. S. Fisher and D. Dever, Trans. Metall. Soc. AIME 239, 48 (1967).
[d]C. P. Kempter, Phys. Status Solidi 8, 161 (1965).
[e]C. W. Garloud and J. Silverman, Phys. Rev. 119, 1218 (1960).
[f]A. R. Miedema, Philips Tech. Rev. 33, 157 (1973).
[g]J. R. Chelikowsky, Phys. Rev. B 19, 686 (1979).

a large difference in electron densities n_{WS} at the boundary of the Wigner-Seitz cell for Cd compared to Ru, Os, and Re. During the alloying process this difference must be smoothed out. Miedema *et al.*[22] showed that n_{WS} is inversely proportional to the atomic volume. A compression of the Cd atom to, for instance, the Os volume increases n_{WS} to 2.76×10^{-2} electrons/a.u.^{3}, insufficient to smooth out the discontinuity. The Cd atom has to be compressed further because charge transfer from Os to Cd is negligible due to the higher electronegativity for Os as compared to Cd. This strong compression of the Cd atom will probably rise the energy and increase the width of the *d* band at the Cd site, invoking an increasing interaction with the *d* electrons of Ru, Os, or Re atoms (Fig. 6). This interaction is very likely responsible for the strong binding of the Cd to the Ru, Os, or Re lattice and is probably of the exchange type due to overlapping *d* shells. The smaller discontinuity of n_{WS} for Cd in Ti, Zr, or Hf can be smoothed out by charge transfer from Ti, Zr, or Hf to the Cd atom. Therefore, the low energetic and well-localized *d* electrons (small bandwidth, Fig. 6) do not interact with the *d* electrons of the host lattice atoms, and consequently, the binding of the Cd atom to the lattice is much weaker, although it is not clear why it is so weak.

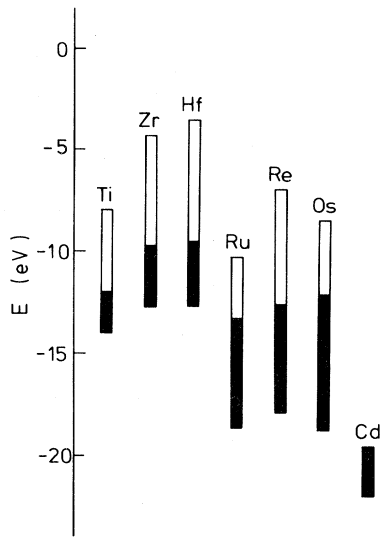

FIG. 6. Energies and bandwidths of the *d* band in the hexagonal transition metals and Cd. The number of electrons in the band is proportional to the black colored surface.

ACKNOWLEDGMENTS

We are very grateful to Professor E. Bucher and Mr. J. Hufnagl of the Universität Konstanz for growing the Ru and Os single crystals. Our thanks are also due to Mr. L. Verwilst and Mr. W. Schollaert for preparing and executing the implantation work. This work was supported by the Interuniversitair Instituut voor Kernwetenschappen.

[1]J. Christiansen, P. Heubes, R. Keitel, W. Klinger, W. Loeffler, W. Sandner, and W. Witthuhn, Z. Phys. B 24, 177 (1976).
[2]W. Bartsch, B. Lamp, W. Leitz, H. E. Mahnke, W. Semmler, R. Sielemann, and Th. Wichert, Z. Phys. B 32, 301 (1979).
[3]H. E. Mahnke, E. Dafni, M. H. Rafailovich, G. D. Sprouse, and E. Vapirev, Phys. Lett. 71A, 112 (1979).
[4]K. Nishiyama and D. Riegel, Hyperfine Interact. 4, 490 (1978).
[5]T. J. Bastow, S. L. Mair, and S. W. Wilkins, J. Appl. Phys. 48, 494 (1977).
[6]R. C. Reno, R. L. Rasera, and G. Schmidt, Phys. Lett. 50A, 243 (1974).
[7]N. Buttler, dissertation, University of Bonn, 1970 (unpublished).
[8]L. Hermans, M. Rots, J. Claes, G. N. Rao, and R. Coussement, Phys. Rev. B 23, 2674 (1981).
[9]L. Hermans, M. Rots, G. N. Rao, R. Coussement, and M. Cogneau, Phys. Rev. B 25, 7474 (1982).
[10]Average value of the following references: R. S. Raghavan, P. Raghavan, and J. M. Friedt, Phys. Rev. Lett. 30, 10 (1973); P. Herzog, K. Freitag, M. Reuschenbach, and H. Walitzki, Z. Phys. A 294, 13 (1980); H. Ernst, thesis, Technische Universität, München, 1979 (unpublished).
[11]T. P. Das and M. Pomerantz, Phys. Rev. 123, 2070 (1961).
[12]F. D. Feiock and W. R. Johnson, Phys. Rev. 187, 39 (1969).
[13]W. B. Pearson, *Handbook of Lattice Spacings and Structures of Metals and Alloys-2* (Pergamon, New York, 1967), p. 835.
[14]V. A. Finkel, M. I. Palatnik, and G. P. Kovtun, Fiz. Met. Metalloved. 32, 212 (1971).
[15]P. S. Raghavan, E. N. Kaufmann, and P. Raghavan, Phys. Rev. Lett. 34, 1280 (1975).
[16]E. Recknagel, A. Weidinger, and R. Wessner, Jahresbericht Universität Konstanz 1978, p. 25 (unpublished).
[17]E. Recknagel (private communication).
[18]W. B. Pearson, *Handbook of Lattice Spacings and Structures of Metals and Alloys-2* (Pergamon, New York, 1967), p. 797.
[19]P. Heubes, W. Keppner, and G. Schatz, Hyperfine Interact. 7, 93 (1979).
[20]T. Butz and W. Potzel, Hyperfine Interact. 1, 157 (1975).
[21]M. H. Rafailovich and G, Schatz, Hyperfine Interact. 9, 315 (1981).
[22]A. R. Miedema, F. R. de Boer, and P. F. de Chatel, J. Phys. F 3, 1558 (1973).